Eph - International Journal Of Science And Engineering
ISSN (Online): 2454-2016
Volume 04 Issue 01 March 2018

DOI:https://doi.org/10.53555/eijse.v4i1.132

FLOW CONTROL AROUND A 3D-BLUFF BODY USING PASSIVE DEVICE

Ankush Raina[1]*, Akhil Khajuria[2]
*[*1] School of Mechanical Engineering, SMVD University, Katra, 182320, J&K, India.*
[2]Department of Mechanical Engineering, NIT Jalandhar, Punjab.

***Corresponding author:-**
Email:- ankush.smvd@gmail.com , Ph.:- +91-9419167410,

Abstract:-
*This article focuses on the flow control around an Ahmed body using deflector plate. The coefficient of drag was obtained numerically for different flow velocities. The study was carried out using a k-ε model for an Ahmed body of 25° rear slant. Grid independence studies were carried out prior to the simulation in order to validate the selected turbulence model. It was observed that coefficient of drag decreases with the increase in flow velocity whereas the lift coefficient increases. A maximum of 13.34 % decrease in drag coefficient was observed for inlet flow velocity of 80 m/***s.**

Keywords: - *Bluff Body, Flow control, Drag coefficient.*

INTRODUCTION

The increasing energy demands and depleting natural resources have forced the researchers to explore different ways by which energy can be saved. Different researchers are being carried out to explore the alternative energy options as well as focus is also on the efficient use of available resources. In automobile sector itself a major chunk of the energy is consumed. Out of the total energy consumption, nearly 2/3rd of the energy is unutilized and is wasted in the form of heat only. For a vehicle plying on road fuel consumption depends on the series of factors in which aerodynamic aspects plays a significant role. Thus the efficiency of a vehicle directly depends on the drag presented by the air [1].

Different research studies carried out in this regard reveal that the rear end of the vehicle plays a significant role in deciding the flow behaviour and hence the coefficient of drag [2]. Different studies made in the wake region reveal that the pair of counter rotating longitudinal vortices and the region of separation bubble dominates the flow around the bodies [3-5]. The flow can be modified by two methods one is by the use of active flow control devices and the other is passive flow control devices. The investigation concerning the active flow control devices was presented by using the different techniques viz. synthetic jets [6], pulsed jets [7, 8] and condo jets [9, 10] where in the capabilities of said flow control techniques were explored by the different authors. The effect of blowing slots at the rear end of the model was evaluated by Roumeas et al [11]. The authors reported a substantial decrease in the size of the wake.

On the other hand the passive flow control devices include the use of splitter plates, flaps, vortex generators. Gillieron and Kourta [12] reported the use of splitter plates wherein the effect on the size and distance of the splitter plates from the bluff body model was evaluated. The flow control by the use of flaps was investigated by Beaudoin and Aider [13]. Authors also analysed the effect of vortex generators for the Ahmad body model. The authors reported that delay in flow separation by the use of vortex generators resulted in the reduction of drag coefficient [14]. A 10 % improvement in the drag coefficient was reported by Pujals et al [15] by using the streaks at the rear end of the Ahmad Body.

The aerodynamic studies are performed to reduce the lift and drag coefficients. This paper is an extension of the previous work wherein the effect of deflector angle on the different inlet flow velocities was presented [16]. In this article, the aim is to explore the effect of additional flow velocities on drag coefficient, but with a different turbulence model ie k-ε model. The model used in this study is the Ahmad Body with a rear slant angle of 25°.

Geometry and grid generation

A 1:4 scale model of Ahmed body with length 1044 mm, width 389 mm and height 288 mm was selected for simulation. At the rear end of the model deflector with a length equal to the width of the Ahmed body was installed. Figure 1 depicts the deflector with the direction of different inclination to be studied. The corners of the deflector are cut at 45° each. Flow simulations are performed in the domain based on the wind tunnel having length 10L, width 2L and height 1.5L, where L is the length of Ahmed body model.

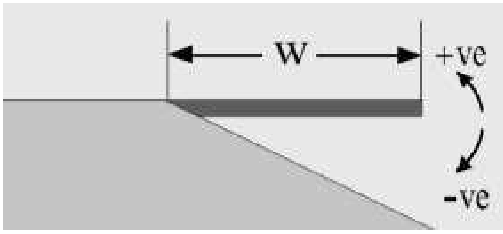

Figure 1: Deflector at rear end of Ahmed body and direction of its inclination.

Grid independence studies were performed to select the optimum number of grid volumes. A sub domain was also created to obtain with fine grid volumes in order to obtain accurate results in the near wall region. The purpose of creating the sub domain is to save the extra time and at the same time to predict the accurate results.

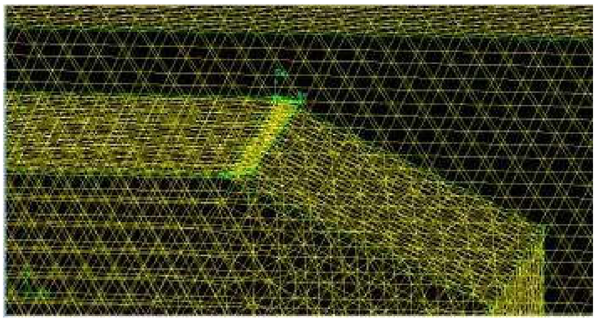

Figure 2: Grid volumes at the rear end of the Ahmed Body

Boundary conditions

The inlet boundary of the flow domain is located at 2.4L times in front of the Ahmed body model where inflow velocity as a boundary condition is prescribed while a constant pressure is imposed at the outlet of the flow domain which is 6.6L away from the rear end of the model. The four sides of the domain are simulated as the walls and surfaces of the model are treated as walls with no slip condition. Different inlet conditions are given in Table 1.

Table 1: Different boundary conditions

1	Inlet velocity	20 m/s, 50 m/s, 80m/s
3	Outlet pressure	0 Pascal
4	Turbulence model	*k-ε*
5	Turbulence kinetic energy	0.001 m^2/s^2
6	Turbulence dissipation rate	0.0001 m^2/s^2

Numerical method

Different models have been proposed over the number of years in order to predict the flow behavior under different operating conditions. Timely advancements have increased the computing ability of these models to predict the values very close to the experimental data. [17].In most the engineering problems, the applications of $k-\varepsilon$ turbulence model are numerous. The standard model is derived for high Reynolds number and is used in conjunction with a wall function when it is applied to wall-bounded turbulent flows. However, a universal function does not exist in complex flow and it is thus necessary to develop a form of $k-\varepsilon$ model equations that can be integrated down to the wall. The original impetus for the $k-\varepsilon$ model was to improve the mixing-length model.

For turbulent kinetic energy *k*,

$$\frac{\partial(\rho k)}{\partial t}+\frac{\partial(\rho k u_i)}{\partial x_i}=\frac{\partial}{\partial x_j}\left[\frac{\mu_t}{\sigma_k}\frac{\partial k}{\partial x_j}\right]+2\mu_t E_{ij}E_{ij}-\rho\varepsilon$$

And for dissipation *ε*,

$$\frac{\partial(\rho\varepsilon)}{\partial t}+\frac{\partial(\rho\varepsilon u_i)}{\partial x_i}=\frac{\partial}{\partial x_j}\left[\frac{\mu_t}{\sigma_\varepsilon}\frac{\partial\varepsilon}{\partial x_j}\right]+C_{1\varepsilon}\frac{\varepsilon}{k}2\mu_t E_{ij}E_{ij}-C_{2\varepsilon}\rho\frac{\varepsilon^2}{k}$$

Results and discussions grid independence studies

The results were obtained by carrying out the grid independence studies in order to select the optimum number of mesh volumes in terms of accuracy and time for convergence. The grid independence studies were carried out for an Ahmed body with a deflector having inclination of -16°. Table 2 gives the data for the grid independence studies carried out corresponding to different number of cell volumes. It was observed that 1270002 number of cell volumes are optimum to perform the further simulations.

Table 2: Grid independence results corresponding to different cell volumes.

S. No.	Number of Cell volumes	Coefficient of Drag (C_D)	% Change
1	185545	0.43376	-
2	306570	0.395	8.93
3	518679	0.37533	4.97
4	713969	0.36125	3.7
5	883985	0.34952	3.17
6	1021867	0.34353	1.71
7	1270002	0.34242	0.32
8	1679009	0.34167	0.21

Drag and lift coefficients

The variation of drag coefficient corresponding to the deflector angles is sown in Figure 3 for different Reynolds number. At the inclination of -25 degree (no deflector) the drag coefficient is nearly 0.32 corresponding to the velocity of 20 m/sec. With the increase in the deflector angle an increase in the drag coefficient can be observed up to inclination of 0 degree. It important to understand that the flow behind the bluff body is governed by wake produced at the rear central portion of the body and by the two longitudinal vortices originating from the trailing edges of the body. The increase in the coefficient of drag in this case is due to the increase in the size of wake zone at the rear end of the body. A sudden decrease in drag coefficient is however observed for an inclination of 5 degree. This decrease in the drag coefficient may be attributed to the fact that the increased wake at the rear end comes in the contact with the two counter rotating vortices, thereby minimizing the drag coefficient for a particular inclination. A further increase in the drag coefficient can be observed beyond the inclination of 5 degree. This is due the further increase in the size of central wake at the rear end of the body. The effect of Reynolds number on coefficient of drag is also considerable. It can be observed that the coefficient of drag decreases with increase in Reynolds number. A maximum of 13.34 % decrease in drag coefficient was observed for a flow velocity of 80 m/s when compared to the velocity of 20 m/s.

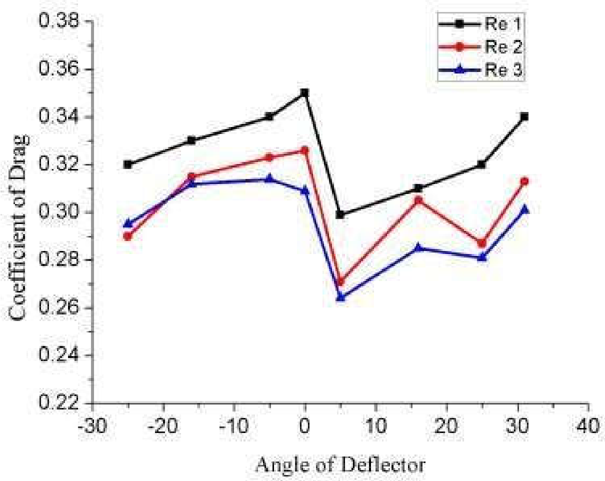

Figure 3: Coefficient of drag corresponding to different Reynolds number

The lift coefficient decreases gradually with the increase in deflector angle till 0 degree (Figure 4). At the inclination of 5 degree a drastic decrease in the lift coefficient is observed. This may be due to the cumulative effect of the increased wake zone and longitudinal vortices. Beyond the inclination of 5 degree an increase in the lift coefficient has been observed. On the other hand, an increase in the lift coefficient has been observed with the increase in the Reynolds number. Thus, from the above discussions it can be ascertained that the drag and lift coefficients are a strong function of deflector angle and Reynolds number.

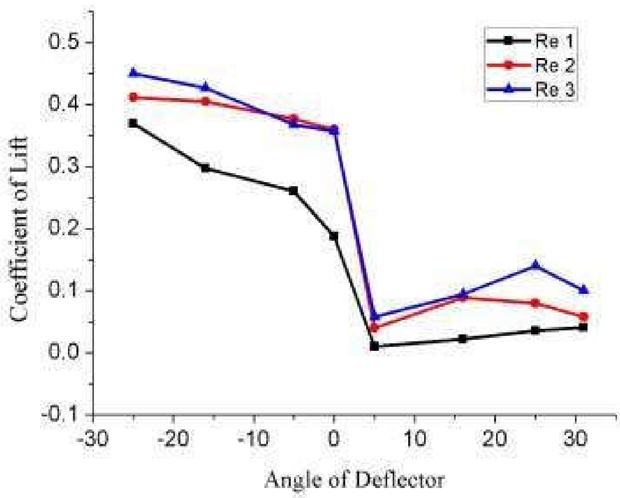

Figure 4: Coefficient of lift corresponding to different Reynolds number

Conclusion

The simulations were performed with an aim to study the effect of Reynolds number on drag and lift coefficients Corresponding to the varying deflector angles. The simulations were carried out using k□□turbulence model. It was observed that coefficient of drag decreases with the increase in the Reynolds number, whereas there is an increase in the lift coefficient. A maximum of 13.34 % decrease in drag coefficient was observed for a flow velocity of 80 m/s. Also, the minimum value of drag coefficient was observed for the deflection inclination of 5 degrees for all the inlet flow velocities considered in the study.

References

[1].Barnard, R. H., 2001 Road vehicle aerodynamic design-an introduction,

[2].Ahmed, S., 1983 Influence of base slant on the wake structure and drag of road vehicles, Journal of fluids engineering, vol. 105, no. 4, pp. 429-434.

[3].Ahmed, S., 1981 Wake structure of typical automobile shapes," Journal of Fluids Engineering, vol. 103, no. 1, pp. 162-169.

[4].Lienhart, H., Becker, S., 2003 Flow and turbulence structure in the wake of a simplified car model, SAE Technical Paper.

[5].Gilliéron, P., Spohn, A., 2002, Flow separations generated by a simplified geometry of an automotive vehicle, IUTAM Symp, Unsteady Separated Flows.

[6].Park, H., Cho, J. H., Lee, J., Lee, D. H., Kim, K. H., 2013 Aerodynamics drag reduction of Ahmed model using synthetic jet array, SAE International Journal of Passenger Cars Mechanical Systems, vol. 6, no. 2013-01-0095, pp. 1-6.

[7].Joseph, P. , Amandolese, X. , Aider, J. L., 2012 Drag reduction on the 25 slant angle Ahmed reference body using pulsed jets, Experiments in Fluids, vol. 52, no. 5, pp. 11691185.

[8].Gillieron, P., kourta, A., 2013 Aerodynamics drag control by pulsed jets on simplified car geometry, Experiments in Fluids, vol. 54, no. 2, pp. 1-16.

[9].Barros, D., Boree, J., Noack, B. R., Sophn, A., Ruiz, T., 2015 Bluff body drag manipulation using pulsed jets and Coanda effect, arXiv preprint arXiv: 1507.02243.

[10]. Khalight, B., Chen, K. H., Iaccarino, G., 2012 Unsteady aerodynamics flow investigation around a simplified aquare-back road vehicle with drag reduction devices, Journal of Fluids Engineering, vol. 134, no. 6, pp. 061101.

[11]. Roumeas, M., Gilliéron, P., Kourta, A., 2009 Analysis and control of the near-wake flow over a squareback geometry, Computers & Fluids, vol. 38, no. 1, pp. 60-70.

[12]. Gilliéron, P., Kourta, A., 2010 Aerodynamic drag reduction by vertical splitter plates, Experiments in fluids, vol. 48, no. 1, pp. 1-16.

[13]. Beaudoin, J.-F., Aider, J.-L., 2008 Drag and lift reduction of a 3D bluff body using flaps, Experiments in fluids, vol. 44, no. 4, pp. 491-501.

[14]. Beaudoin, J.-F., Aider, J.-L., Winfried, J. E., 2010 Drag and lift reduction of a 3D bluff body using active vortex generators," Experiments in fluids, vol. 48, no. 5, pp. 771-789.

[15]. Pujals, G., Depardon, S., Cossu, C., 2010, Drag reduction of a 3D bluff body using coherent streamwise streaks, Experiments in fluids, vol. 49, no. 5, pp. 1085-1094.

[16]. Raina, A., Harmain, G.A. and Haq, M.I.U., 2017. Numerical investigation of flow around a 3D bluff body using deflector plate. International Journal of Mechanical Sciences, 131, pp.701-711.

[17]. Menter, F. R., 1992 Performance of popular turbulence model for attached and separated adverse pressure gradient flows, AIAA journal, vol. 30, no. 8, pp. 2066-2072.